

# Cockscomb-like fibrous silica beta zeolite (FSBEA) as a new engineered catalyst for enhanced CO methanation

I Hussain<sup>1</sup>, A A Jalil<sup>2,3\*</sup>, N A A Fatah<sup>2</sup>, S M Izan<sup>1</sup> and M S Azami<sup>1</sup>

<sup>1</sup>Faculty of Science, Universiti Teknologi Malaysia, 81310 UTM Johor Bahru

<sup>2</sup>School of Chemical and Energy Engineering, Faculty of Engineering, Universiti Teknologi Malaysia, 81310 UTM Johor Bahru, Johor, Malaysia

<sup>3</sup>Centre of Hydrogen Energy, Institute of Future Energy, 81310 UTM Johor Bahru, Johor, Malaysia

\*aishahaj@utm.my

**Abstract.** This study focuses on the synthesis of cockscomb-like fibrous silica beta zeolite (FSBEA) and its application in CO methanation to produce substituted natural gas (SNG). FSBEA was synthesized by microemulsion technique using commercial beta zeolite-seeds and characterized by FESEM, XRD, N<sub>2</sub> physisorption and FTIR spectroscopy. The results showed that the FSBEA had a unique cockscomb-like morphology with particle size 400-800 nm, enhanced interparticle porosity and high BET surface area of 532 m<sup>2</sup>/g, which offers more adsorption sites for the CO and H<sub>2</sub> molecules to enhance CO methanation activity. Catalytic performance results revealed that FSBEA demonstrated higher CO conversion (71%), selectivity (64%), the yield of CH<sub>4</sub> (46%) and the rate of CH<sub>4</sub> formation (0.0375 μmol-CH<sub>4</sub>/m<sup>2</sup>s) than commercial based BEA. Besides, FSBEA expressed high thermal stability up to 45 h during CO methanation at 450 °C. Therefore, this study offers an attractive and sustainable route for SNG over FSBEA that may be used as a clean and alternate energy source for fossil fuels.

## 1. Introduction

Among the fossil fuels, natural gas has more potential due to its ready availability, slag, and smoke-free composition, low sooting tendency, and high calorific value. Natural gas is the fastest-growing energy source of the world [1-2]. Recently, the production of substituted natural gas (SNG) has attracted much attention due to exhaustion and the rising price of natural gas, particularly in those regions which are deficient in natural gas and rich with coal reservoirs such as China [3]. SNG has many applications. It can be used in gas turbines, gas engines, and the transportation sector, such as in vehicles. SNG can be distributed by the existing gas pipeline and storage tanks [4-5]. SNG gas has been produced from coal, renewable biomass via syngas (H<sub>2</sub>+CO). The process consists of the coal gasification chamber, acid gas removal chamber, CO methanation chamber, and thermal power station for supplying steam and power. Among them, CO methanation is one of the most crucial steps during the production of SNG. It is also known as the Sabatier reaction, discovered by Sabatier since 1902. CO methanation also used to remove the trace amount of CO from H<sub>2</sub>-rich feed gas, which used in fuel cells later and NH<sub>3</sub> synthesis process as well as Fischer-Tropsch synthesis [6-7].

However, CO methanation is a highly exothermic reaction; one of the serious problems of this reaction is a significant loss of catalytic activity with time due to coke deposition and metal sintering. To address these issues, several studies have been conducted on the development of appropriate CO



methanation catalysts using various type of metal including Mo, Fe, Ni, Co, Pt, Rh and Ru on different supports ( $\text{Al}_2\text{O}_3$ ,  $\text{SiO}_2$ ,  $\text{TiO}_2$ ,  $\text{ZrO}_2$  or mixed oxides) [8]. However, the challenges related to the best choice of an efficient and suitable catalyst have still remained, especially supported material. Zeolite based materials have attracted much attention from researchers. Particularly, in the field of heterogeneous catalysis. Furthermore, zeolites are used in various reactions as active supports such as isomerization, cracking, alkylation and aromatization of hydrocarbons due to unique properties own their high activity, shape selectivity, ion exchanging properties and special pore structure. However, zeolites have some limitations as well that affect their catalytic performance [9- 11]. Due to the limited size of the channels, cavities and the lack of interconnectivity. Particularly, mordenite, ZSM-5, Y zeolite, and beta zeolite that own relatively microporous nature and diffusion limitation problem in many catalytic reactions, which lead to coke formation and catalyst deactivation [12]. Development of mesopores in microporous zeolites has provided the best solution to overcome diffusion limitation and pore blockage that conventional zeolites face [13].

A prodigious initiative was taken by Polshettiwar et al. in 2010 in the field of fibrous material. The first fibrous material KCC-1 was synthesized with high surface area and better accessibility of active site [14]. Later, in several studies, KCC-1 was used in various reactions, such as  $\text{CO}_2$  methanation [15], isomerization [16]. The microemulsion technique was used to develop silica-based fibrous materials [17]. Fibrous silica ZSM-5 was initially synthesized by Firmansyah et al. in 2016 that was used for cumene hydrocracking [18]. Fibrous based-zeolites are believed to have much potential in enhancing the catalytic performance of isomerization, [19], CO methanation [20], and petrochemical processes [21]. Thus, the employment of fibrous zeolite may improve the catalytic performance of CO methanation. Therefore, as an extension of this study, we prepared Cockscomb-like fibrous silica BEA zeolite (FSBEA), which may possess high surface area, high pore volume to enhance CO methanation activity. It may possess a higher number of oxygen vacancies and unpaired electrons that leads to an increase in the catalytic activity.

## 2. Experimental

### 2.1. Catalyst preparation

Cockscomb-like fibrous silica beta zeolite (FSBEA) support was synthesized by microwave-assisted hydrothermal approach. 4.42 g of urea and 6.2 g of cetyltrimethylammonium bromide (CTAB) were dissolved in 163 mL of distilled water. The solution mixture was stirred for 20 min at room temperature to ensure complete mixing. Toluene (170 mL) and butanol (6.5 mL) were added to aqueous mixture solution, followed by stirring for 30 min at room temperature. Beta zeolite seeds (130 g) were added in the solution and stirred for another 20 min. Then tetraethyl orthosilicate (TEOS, 13.15 mL) was added to the mixture and transferred into a Teflon bottle and was stirred for 3 h at room temperature. Afterward, the Teflon bottle containing a milky solution was subjected in an oven at 120 °C pre-aging. After 6 h it was removed from the oven and centrifuged, washed with acetone and dry it at 120 °C for overnight by placing in the oven. Furthermore, the attained white solid was crushed and calcined in a furnace at 550 °C for 6 h to yield the cockscomb-like fibrous silica beta zeolite (FSBEA) support. BEA and FSBEA symbols were used for commercial and as-synthesized catalysts, respectively.

### 2.2. Characterization

Both samples were studied by The X-rays powder diffractometer (Bruker Advance D840 kV) using  $\text{Cu K}\alpha$  as a source of radiation in the range of a  $2\theta$  angle (5-85°) with the wavelength of 1.544 Å using 0.1 scan rate. Fourier-transform infrared (FTIR) spectroscopy was employed using KBr on both samples in scan range of 400-4000  $\text{cm}^{-1}$  on an Agilent FTIR spectrometer (Cary 640). Microscopic surface morphology for both catalysts were analyzed by field emission scanning (FESEM). The  $\text{N}_2$  physisorption analysis was performed by Beckman Coulter SA 3100 equipment using  $\text{N}_2$  adsorption-desorption to investigate the Brunauer-Emmett-Teller (BET) surface area, total pore volume at -196 °C. In addition, pore size distribution was measured through non-local density functional theory (NLDFT)

method. The catalysts were evacuated first at 300 °C for 1 h before being subjected to the adsorption-desorption of N<sub>2</sub>.

### 2.3. Catalytic performance

To perform CO methanation, a fixed-bed quartz reactor employed. Before to run the reaction, each catalyst of 0.2 g was heated in presence of air for 1 h at 500 °C and reduced in H<sub>2</sub> steam of 10 mL/min for 3 h at same temperature. The temperature was adjusted to the 150 °C. The feed gases (CO and H<sub>2</sub>) were injected to fixed bed quartz reactor using 1:5 mass ratio at 0.1 MPa. A gas chromatograph (GC; 6090N Agilent Gas Chromatograph) was connected to thermal conductivity detector (TCD) to measure the composition of the outlet gases during catalytic performance. The following formulae were used to measure the products, in form of the CO conversion, selectivity and rate of formation and yield of methane:

$$X_{CO} (\%) = \frac{M_{CH_4} + M_{CO_2}}{M_{CO} + M_{CH_4} + M_{CO_2}} \times 100 \quad (1)$$

$$S_{CH_4} (\%) = \frac{M_{CH_4}}{M_{CH_4} + M_{CO_2}} \times 100 \quad (2)$$

$$S_{CO_2} (\%) = \frac{M_{CO_2}}{M_{CH_4} + M_{CO_2}} \times 100 \quad (3)$$

$$Y_{CH_4} (\%) = \frac{X_{CO} \times S_{CH_4}}{100} \quad (4)$$

$$Y_{CO_2} (\%) = \frac{X_{CO} \times S_{CO_2}}{100} \quad (5)$$

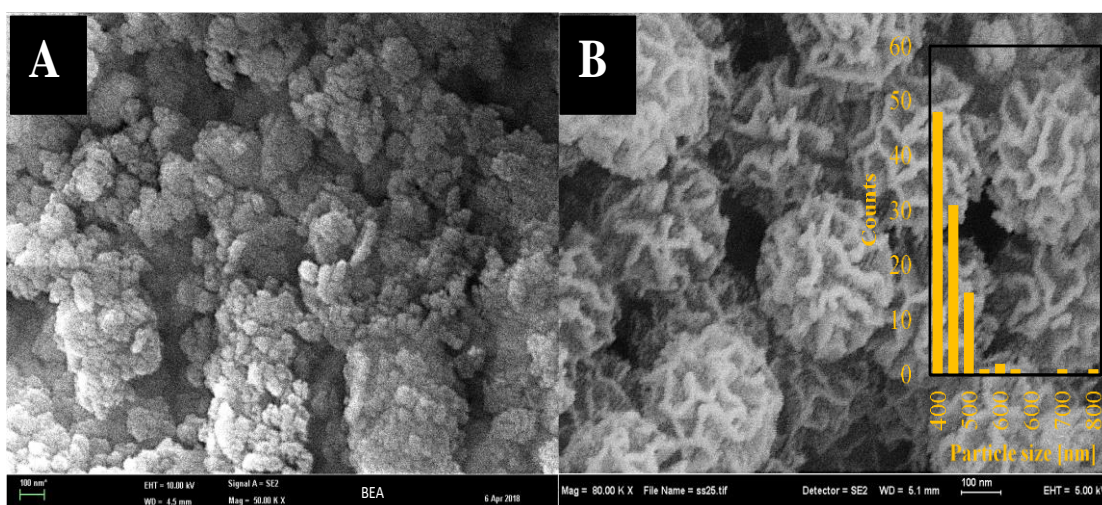
$$\text{Rate of } CH_4 \text{ formation (mmol m}^{-2} \text{ s}^{-1}) = \frac{n_{CH_4}}{W_{cat} \times s} \quad (6)$$

In these equations,  $X_{CO}$  is the CO conversion,  $S_{CH_4}$  is the selectivity,  $Y_{CH_4}$  is the methane yield and  $M$  is the number of moles of CO, CH<sub>4</sub> and CO<sub>2</sub>.  $W$  is the weight of catalysts and  $s$  is time in second

## 3. Results and discussions

### 3.1. Morphological, crystallinity and textural studies

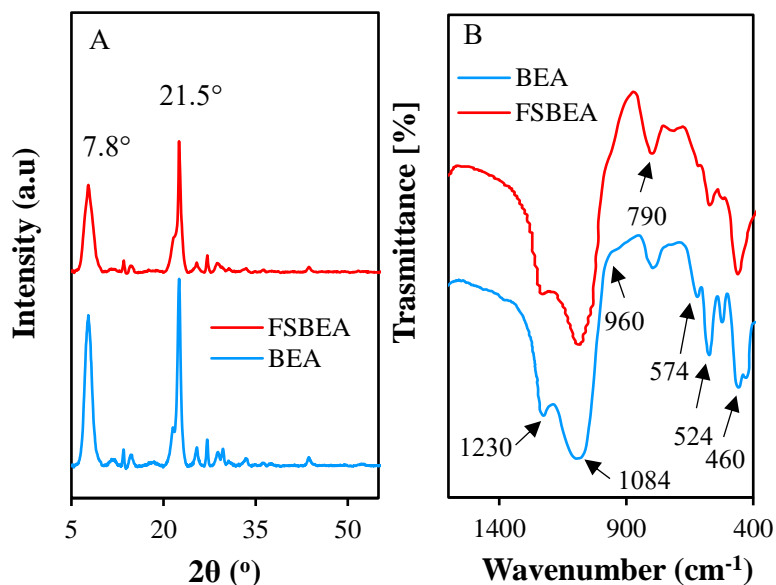
Figure 1 presents the microscopic study of both commercial BEA zeolite and as-synthesised FSBEA. It shows that FSBEA was synthesised successfully from commercial BEA. It is worth noting that clusters of irregular particles (Figure 1A) were changed to unique and well-developed nanospheres (400-800 nm) analogous to well-ordered cockscomb-like morphology of FSBEA (Figure 1B). It looks similar to the KCC-1 structure that was synthesized first time by Polshettiwar *et al.* in 2010 [14]. This tremendous configuration of FSBEA could be effective later, leading to improved surface area and pore size for enhanced CO methanation.



**Figure 1.** FESEM images of (A) BEA and (B) FSBEA.

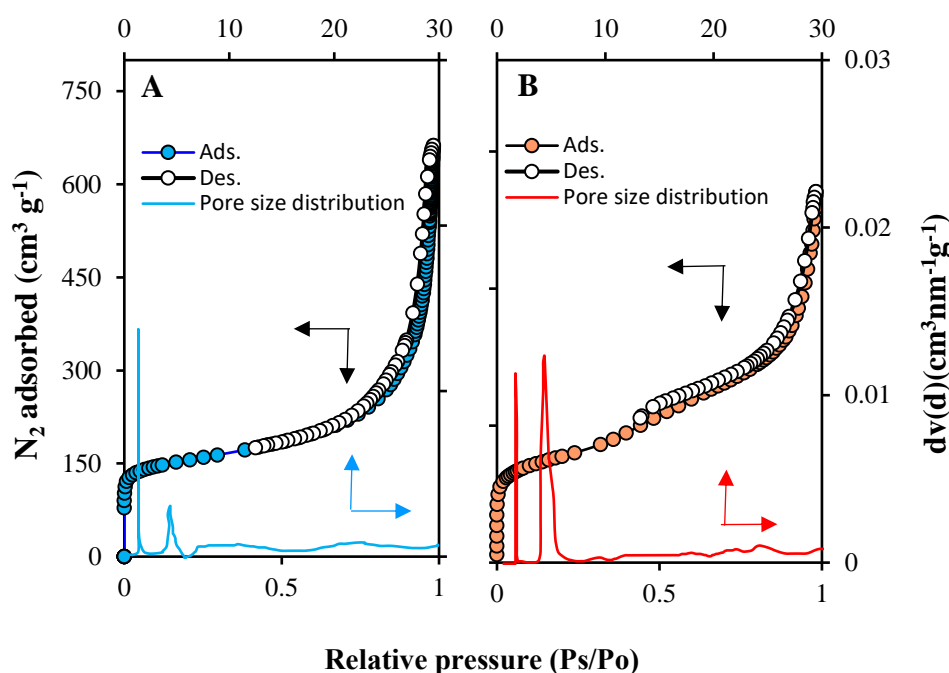
Figure 2A displays the XRD diffractogram of the commercial BEA and FSBEA catalysts. Several peaks were noticed at  $2\theta = 7.8^\circ, 21.5^\circ, 27.2^\circ, 29.9^\circ,$  and  $43.6^\circ$ . It should be noted that the characteristic peaks of FSBEA were similar to the peaks of BEA, which reflected as-synthesized FSBEA without any significant change (JCPDS file No. 00-004-0477) [21]. However, in the case of FSBEA, a substantial loss of crystallinity was observed, particularly at  $2\theta = 7.8^\circ$  and  $21.5^\circ$ , which implied the growth of silica species around the core-shell of BEA. A similar phenomenon was noticed in fibrous silica beta zeolite (FSB) [21], protonated fibrous silica@BEA zeolite [19] and fibrous silica ZSM-5, where the XRD intensity decreased due to high silica growth over the core-shell [18].

Figure 2B shows the FTIR spectra in the range of  $1600\text{--}400\text{ cm}^{-1}$  region. A series of vibrational bands appeared at  $1230\text{ cm}^{-1}, 1084\text{ cm}^{-1}, 960\text{ cm}^{-1}, 790\text{ cm}^{-1}$  and  $574\text{ cm}^{-1}, 524\text{ cm}^{-1}$  and  $460\text{ cm}^{-1}$ . The first four bands ( $1230\text{ cm}^{-1}, 1084\text{ cm}^{-1}, 790\text{ cm}^{-1}$  and  $460\text{ cm}^{-1}$ ) expressed to external and internal asymmetric stretching, symmetric and bending vibrations of T-O-T in the framework, respectively [21]. The band at  $960\text{ cm}^{-1}$  is ascribed to the external SiOH group [25]. The bands  $574\text{ cm}^{-1}$  and  $524\text{ cm}^{-1}$  indicated the presence of 5- and 6-membered rings of the zeolite [26]. These results confirmed the successful synthesis of FSBEA without any significant change.



**Figure 2.** (A) XRD diffractogram and (B) FTIR spectra of BEA and FSBEA.

Figure 3 illustrates the  $\text{N}_2$  physisorption isotherms of BEA and FSBEA catalysts. Both samples revealed Type IV isotherms with the  $\text{H}_3$  hysteresis loop. According to the IUPAC classification, this is the characteristic of mesoporous materials [22]. It is worth noting that  $\text{N}_2$  adsorption at lower ( $P/P_0 = 0 - 0.2$ ) indicated the presence of micropores. Whereas,  $\text{N}_2$  adsorption at higher relative pressure ( $P/P_0 = 0.8 - 1.0$ ) presented mesopores [24]. In addition, the  $\text{N}_2$  adsorption in FSBEA at  $P/P_0 = 0.3-0.4$  and  $P/P_0 = 0.9$  were due to intra- and interparticle porosity, respectively [23]. As a result of FSBEA, it showed a higher surface area of  $532 \text{ m}^2/\text{g}$ ) as compared to commercial BEA ( $407 \text{ m}^2/\text{g}$ ), listed in table 1. The narrow range pore size distribution derived by NLDFT showed a sharp peak in the range of 4 nm to 7.2 nm and 20 nm to 25 nm corresponded to the presence of mesopore in FSBEA. It might be due to the self-assembly of surfactant. Whereas, the small peaks due to mesopores formed by the distance between the silica lamellar structures [19, 23]. These observations are highly in line with the FESEM results.



**Figure 3.** N<sub>2</sub> adsorption-desorption isotherms and NLDFT pore size distribution of (A) BEA and (B) FSBEA.

**Table 1.** physicochemical properties of the catalyts.

Catalysts	Surface area <sup>a</sup> m <sup>2</sup> /g	Total pore volume <sup>a</sup> cm <sup>3</sup> /g	Mesopore volume <sup>b</sup> cm <sup>3</sup> /g	Micropore volume <sup>a</sup> cm <sup>3</sup> /g
FSBEA	532	1	0.91	0.09
BEA	407	0.61	0.47	0.14

<sup>a</sup> Determine from BET and non-local density functional theory (NLDFT)

<sup>b</sup> Total pore volume-micropore volume by t-plot method

### 3.2. Catalytic performance of CO methanation activity

Figure 4 demonstrates catalytic performance for CO methanation activity. It was noticed that both BEA and FSBEA catalysts demonstrated lower performance below 250 °C. It is worth noting that catalytic activity was improved with subsequent heating higher temperatures (350–450 °C) and reached a maximum value at 450 °C. FSBEA showed CO conversion 71 % and methane selectivity 64%. Whereas, BEA showed CO conversion 57 % and 55 % methane selectivity (Figure 4AB). Besides, in terms of the rate of formation of CH<sub>4</sub>, FSBEA demonstrated 0.0375 mmol m<sup>-2</sup> s<sup>-1</sup> higher than BEA (0.0225 mmol m<sup>-2</sup> s<sup>-1</sup> figure 4C). It was observed that at a higher temperature (500 °C) catalytic activity decreased and chemical reactions showed the tendency to attain equilibrium (Figure 4AB). This may be due to the occurrence of a water gas shift reaction (WGS), which is the most common side reaction during CO methanation. To compare these experimental values, we calculated theoretical equilibrium lines for CO conversion and CH<sub>4</sub> selectivity using the HSC Chemistry software 6.0 package at the same conditions of experimental catalytic performance. It should be noted that CO conversion and CH<sub>4</sub> selectivity were consistent with theoretical equilibrium lines at high temperature. Which indicates that thermodynamically, experimental values are within the possible range. CO<sub>2</sub> was produced as a by-

product during WGS reaction. It was seen that an increase in temperature produces more  $\text{CO}_2$ , as shown in figure 4E. CO methanation is generally performed in the presence of metal on support material, which acts as active sites to interact and adsorb the CO and  $\text{H}_2$  molecules. In this study we suggest that intra- and inter-particle porosity in as-synthesized catalyst FSBEA is the main key factor to enhance the CO methanation activity. Similar studies have been conducted on metal-free fibrous supports for CO methanation, where a comparative study was tabulated in table 2. Moreover, thermal stability analysis was conducted at 450 °C for a 65 h time span, and figure 4F specifies that BEA showed deactivation after 31 h, 'where FSBEA demonstrated high thermal stability of 43 h under the same condition'.

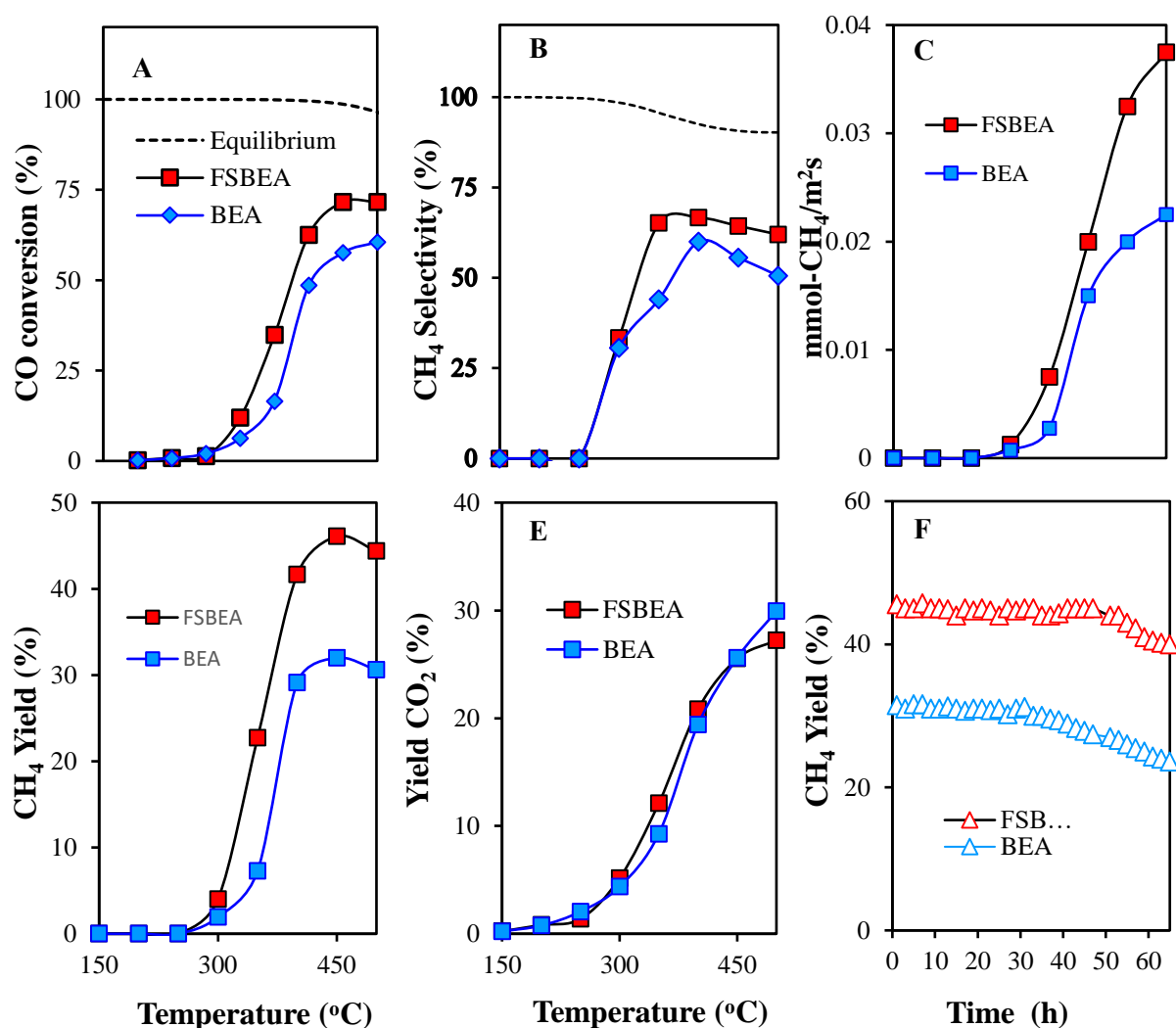


**Figure 4.** (A) CO conversion, (B) Selectivity of methane (C) Rate of formation of methane, and (D) CH<sub>4</sub> yield, (E) CO<sub>2</sub> yield and (F) Thermal stability at 450 °C for BEA and FSBEA. Equilibrium line (dash line) calculated by HSC Chemistry 6 software.

**Table 2.** Comparison study of catalytic activities towards CO methanation.

Catalysts	Reaction Temperature (°C)	CO conversion (%)	CH <sub>4</sub> selectivity (%)	CH <sub>4</sub> Yield (%)	Stability (time/h)	Ref.
FSBEA	450	71	64	46	47	This study
BEA	450	57	55	33	31	This study
FmZSM-5	450	63	69	44	50	[20]
Ni/ $\alpha$ -Al <sub>2</sub> O <sub>3</sub>	450	61	68	42	50	[27]
mZSM-5	450	62	71	43	30	[28]
MoO <sub>3</sub> /Si-ZrO <sub>2</sub>	550	63	59	37	5	[29]

#### 4. Conclusion

This study revealed a remarkable catalytic performance of cockscomb-like fibrous silica BEA zeolite, which was synthesized by the microemulsion system and characterized by FESEM, XRD, N<sub>2</sub> physisorption, and FTIR spectroscopy. The obtained encouraging results discovered that FSBEA had a high surface area, total pore volume, and mesoporosity. FSBEA showed 71 % of CO conversion, 64% of methane selectivity and 0.0375 mmol m<sup>-2</sup> s<sup>-1</sup> of formation of methane with 43 h thermal stability. Catalytic performance results proved that cockscomb-like morphology played a key role to enhance CO methanation. It is suggested that FSBEA can be an effective catalyst in heterogeneous base-catalyzed reactions. Particularly, in CO hydrogenation catalysts for industrial applications. It presents an attractive and sustainable route for production SNG, which can be used as a clean and alternate energy source for fossil fuels.

#### Acknowledgments

This research work was supported by the Transdisciplinary Research Grant from Universiti Teknologi Malaysia (Grant No. 06G52 and 06G02) and the Fundamental Research Grant Scheme from the Ministry of Higher Education, Malaysia (Grant No. FRGS/1/2017/STG07/UTM/01/1).

#### References

- [1] Shu-S.L, Yong-Y. J, Yahong H, Jinxian Z and Jun R 2018 *Fuel Process. Technol.* **177** 266
- [2] Fanhui M, Xin L, Xiaoyang L and Zhong L 2018 *Int. J. Coal Sci. Technol.* **4** 439
- [3] Dandan G, Shuangshuang L, Shaoxia G, Honggui T, Hong W and Yuan L 2018 *Appl. Surf. Sci.* **434** 351
- [4] Romel J, Karla F, Mari P, M, Sebastian G, Francisco G and Alejandro K 2019 *I. Int. J. Hydrogen Energ.* **44** 768
- [5] Hiroyuki K, Zhi Q. T, Yoshinori I, Catherine K S. C, Jie C, Martin S, Luwei C and Armando B 2018 *Catal. Today* **299** 193
- [6] Shuangshuang L, Honggui T, Dandan G, Zhi M and Yuan L 2017. *Catal. Today* **297** 298
- [7] Jun R, Haidong L, Yongyong J, Jiyu Z, Shusen L, Jianying L and Zhong L 2017 *Appl. Catal. B- Environ.* **201** 561
- [8] Ahmad E, Somayeh T and Farhad K 2018 *Ind. Eng. Chem. Res.* **5738** 12700
- [9] Wang L, Yin C, Shan Z, Liu S, Du Y and Xiao F 2009 *Colloid Surf. A-Physico-chem. Eng. Asp.* **340** 126
- [10] Rahimi N and Karimzadeh R 2011 *Appl. Catal. A.* **398** 1
- [11] Frederic S, Irin S, Sonia A, Adriana B, Karine T, Christian F, Jean G and Javier R 2009 *J Catal* **264** 11
- [12] Mariusz G, Lukasz K, Jerzy P, Bogdan S and Jerzy D 2018 *Spectrochim Acta. A Mol. Biomol. Spectrosc.* **193** 440
- [13] Meng X, Nawaz F and Xiao F 2019 *Nano Today* **4** 292



- [14] Polshettiwar V, Cha D, Zhang X and Basset J.M 2010 *Angew Chemie-Int. Ed.* **49** 52
- [15] Hamid M.Y.S, Triwahyono S, Jalil A.A, Jusoh N.W.C, Izan S.M and Abdullah T.A.T 2018 *Inorg. Chem.* **57** 5859
- [16] Fatah N.A.A, Triwahyono S, Jalil A.A, Salamun N, Mamat C.R and Majid Z.A. *Chem. Eng. J* **314** 650
- [17] Moon D. S and Lee, J. K 2012 *Langmuir* **28** 12341
- [18] Firmansyah M.L, Jalil A.A, Triwahyono S, Hamdan H, Salleh M.M, Ahmad W.F.W and Kadja G. T. M. 2016 *Catal. Sci. Technol.* **6** 5178
- [19] Izan S.M, Triwahyono S, Jalil A.A, Majid Z.A, Fatah N.A.A, Hamid M.Y.S and Ibrahim M 2019 *Appl. Catal. A Gen.* **570** 228
- [20] Teh L.P, Triwahyono S, Jalil A.A, Firmansyah M.L, Mamat C.R and Majid Z.A 2016 *Appl Catal A: Gen.* **523** 200
- [21] Ghani N.N.M, Jalil A.A, Triwahyono S, Aziz M.A.A, Rahman A.F.A, Hamid M.Y.S, Izan S.M and Nawawi M.G.M 2019 *Chem. Eng. Sci.* **193** 217
- [22] Rahman A.F.A, Jalil, A.A, Triwahyono S, Ripin A, Aziz F.F.A, Fatah N.A.A, Jaafar N.F, Hitam C.N.C, Salleh N.F.M and Hassan N.S 2017 *Clean. Prod.* **143** 948
- [23] Hamid M.Y.S, Firmansyah M.L, Triwahyono S, Jalil A.A, Mukti R.R, Febriyanti E, Suendo V, Setiabudi H.D, Mohamed M and Nabgan W 2017 *Appl. Catal. A Gen.* **532** 86
- [24] Thommes M, Katsumi K, Alexander V.N, James P. O, Francisco R.R, Jeans R and Kenneth S.W.S 2015 *Pure Appl. Chem.* **87** 1051
- [25] Jusoh N.W.C, Jalil A.A, Triwahyono S, Karim A.H, Salleh N.F, Annuar N.H.R, Jaafar N.F, Firmansyah M.L, Mukti R.R and Ali M.W 2015 *Appl. Surf. Sci.* **330** 10
- [26] Fathi S, Sohrabi M and Falamaki C 2014 *Fuel* **116** 529
- [27] Jiajian G, Chunmiao J, Meiju Z, Fangna G, Guangwen X and Fabing S 2013 *Catal. Sci. Technol.* **3** 2009
- [28] Teh L.P, Triwahyono S, Jalil A.A, Mukti R.R, Aziz M.A.A and Shishido T 2015 *Chem. Eng. J.* **270** 196
- [29] Jia Gu, Zhong Xin, Miao Tao, Yuhao Lv, Wenli Gao and Qian Si 2019 *Appl. Catal. A: Gen.* **575** 230